The Journal of Chemical Physics

Reactive Monte Carlo simulations for charge regulation of colloidal particles

Cite as: J. Chem. Phys. **156**, 014108 (2022); https://doi.org/10.1063/5.0077956
Submitted: 08 November 2021 • Accepted: 10 December 2021 • Accepted Manuscript Online: 13 December 2021 • Published Online: 03 January 2022

Amin Bakhshandeh, Derek Frydel and Yan Levin

The Journal of Chemical Physics ARTICLE scitation.org/journal/jcp

Reactive Monte Carlo simulations for charge regulation of colloidal particles

Cite as: J. Chem. Phys. 156, 014108 (2022); doi: 10.1063/5.0077956
Submitted: 8 November 2021 • Accepted: 10 December 2021 •
Published Online: 3 January 2022

Amin Bakhshandeh,[1,a] Derek Frydel,[2,b] and Yan Levin[1,c]

AFFILIATIONS

[1] Instituto de Física, Universidade Federal do Rio Grande do Sul, Caixa Postal 15051, CEP 91501-970 Porto Alegre, RS, Brazil
[2] Department of Chemistry, Universidad Técnica Federico Santa María, Campus San Joaquin, 7820275 Santiago, Chile

[a] Electronic mail: amin.bakhshandeh@ufrgs.br
[b] Electronic mail: derek.frydel@usm.cl
[c] Author to whom correspondence should be addressed: levin@if.ufrgs.br

ABSTRACT

We use a reactive Monte Carlo simulation method and the primitive model of electrolyte to study acid–base equilibrium that controls charge regulation in colloidal systems. The simulations are performed in a semi-grand canonical ensemble in which colloidal suspension is in contact with a reservoir of salt and strong acid. The interior of colloidal particles is modeled as a low dielectric medium, different from the surrounding water. The effective colloidal charge is calculated for different numbers of surface acidic groups, pH, salt concentrations, and types of electrolyte. In the case of potassium chloride, the titration curves are compared with the experimental measurements obtained using potentiometric titration. A good agreement is found between simulations and experiments. In the case of lithium chloride, the specific ionic adsorption is taken into account through the partial dehydration of lithium ion.

I. INTRODUCTION

The interplay between electrostatic interactions[1–21] and acid–base equilibrium is of paramount importance in chemistry and biology.[22–27] It often defines the boundary between life and death. The protein functionality can change due to the modification of surrounding pH, affecting the enzymatic activity and the resulting metabolic processes.[28] The transport of ions through the cellular membranes[29] is strongly affected by pH. The same is true for the binding of heavy metals to bacterial membrane.[30–32] In biological systems, pH, which depends on the activity of proton inside the solution, can be significantly modified by the presence of an electrolyte, which at physiological concentration is around 150 mM,[33,34] affecting the solubility and stability of proteins.[27,34–45] In colloidal science, both pH and electrolyte concentrations regulate colloidal charge and interaction between the particles.[13,16,46,47]

In the present paper, we will use reactive Monte Carlo simulation to efficiently explore the effective charge of colloidal particles inside an electrolyte solution of a given pH. Differently from constant pH simulations,[38,39] we treat all ions, including hydronium, explicitly in the semi-grand canonical ensemble. The advantage of this approach is that it automatically enforces uniform electrochemical potential of all ions inside the simulation cell.[48–53] In this respect, our approach is similar to other recently introduced grand canonical simulation methods to account for charge regulation.[48,53–57] The explicit treatment of all ions makes our method quite general. It can be easily modified to treat surfaces with basic groups as well as surfaces composed of both basic and acidic groups. Furthermore, we can also include specific adsorption of ions to charged surface groups. The implementation that we present in the present paper, which relies on the accurate analytical expressions for the excess ionic chemical potential available in the literature, makes our simulation method computationally efficient.

This article is organized as follows: In Sec. II, we introduce and describe the system. In Sec. III, we discuss the simulation method. In Sec. IV, we compare the simulation method with the experimental results. In Sec. V, we consider the scenario in which a cation K^+ is substituted by Li^+, which can specifically adsorb to carboxylate. The work is concluded in Sec. VI.

II. MODEL AND SYSTEM DETAILS

The system consists of a single colloidal particle of radius a fixed at the center of a spherical Wigner–Seitz (WS) cell whose radius R determines the volume fraction of the colloidal suspension of a

corresponding experimental system. The cell is allowed to exchange ions with a reservoir containing strong monovalent salt and acid, at concentrations c_s and c_a, respectively, both of which fully dissociate in an aqueous solution (see Fig. 1). All ions have charge $\pm q$, where q is the proton charge. The dielectric constant inside the colloidal sphere, representing a polystyrene latex particle, is $\epsilon_c \approx 2.5$, while the dielectric constant of the surrounding water is $\epsilon_w \approx 80$. One advantage of working with the WS formalism is that the contact theorem allows us to calculate the osmotic pressure inside the colloidal suspension directly using ionic densities at contact with the cell boundary.[58]

The colloidal surface contains acidic groups of weak acid that only partially dissociate upon contact with an aqueous solution: the process is governed by the reaction $HA \rightleftharpoons H^+ + A^-$ and the corresponding dissociation constant K_a. These surface groups are modeled as small spheres of radius $r_0 = 2$ Å randomly distributed over the colloidal surface. The dielectric constant of small spheres is the same as that of water, so that dielectric discontinuity occurs only at the colloidal boundary. The choice to keep the smaller spheres lying on the colloidal surface rather than embedded into it has a physical motivation. Charged surface groups prefer being displaced from the region of low dielectric constant. The acidic surface groups are also referred to as titration sites. In its deprotonated state, a titration site has charge $-q$, and in a protonated state, it has charge 0 (see Fig. 1). The charge of the titration site is located at its center.

The region outside the colloidal particle is occupied by the ions of a fully dissociated strong salt and acid, $KCl \rightarrow K^+ + Cl^-$ and $HCl \rightarrow H^+ + Cl^-$. All ions are represented by hard spheres of radius 3.3 Å,[59] corresponding to fully hydrated ions. In particular, a proton H^+ does not exist separately but is a hydronium ion, H_3O^+.

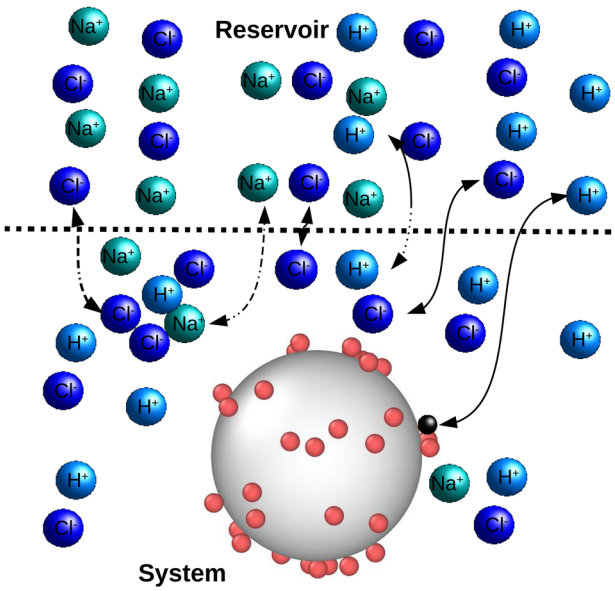

FIG. 1. Schematic representation of reactive MC moves. The deprotonated acidic groups A^- randomly distributed over the colloidal surface are represented by the red spheres and protonated HA groups are represented by the black spheres. The protonation of a titration site, $A^- + H^+ \rightarrow HA$, changes its charge from $-1q \rightarrow 0$; at the same time, Cl^- is added to the cell with grand canonical probability, to preserve the overall charge neutrality. Deprotonation reaction, $HA \rightarrow A^- + H^+$, results in the change $0 \rightarrow -1q$ of the titration site and simultaneous removal of Cl^- from the simulation cell.

The dielectric contrast between the colloidal core and the surrounding water results in induced surface charge density at the interface. The surface charge distribution depends on the location of ions inside the suspension. Therefore, the interaction between any two ions near a colloidal particle will not be given simply by the Coulomb potential but will also depend on their distance from the colloidal surface. The Green function for the effective interaction between two ions inside the WS cell is accurately approximated by[60–62]

$$G(\mathbf{r},\mathbf{r}') = \frac{1}{\epsilon_w|\mathbf{r}-\mathbf{r}'|} + \frac{\gamma a}{\epsilon_w r'|\mathbf{r}-\frac{a^2}{r'^2}\mathbf{r}'|} + \gamma\psi_c(\mathbf{r},\mathbf{r}') \tag{1}$$

with

$$\psi_c(\mathbf{r},\mathbf{r}') = \frac{1}{\epsilon_w a}\ln\left[\frac{rr' - \mathbf{r}\cdot\mathbf{r}'}{a^2 - \mathbf{r}\cdot\mathbf{r}' + \sqrt{a^4 - 2a^2(\mathbf{r}\cdot\mathbf{r}') + r^2r'^2}}\right], \tag{2}$$

where $\gamma = (\epsilon_w - \epsilon_c)/(\epsilon_w + \epsilon_c)$. The first term of Eq. (1) is due to the direct Coulomb potential produced by an ion located at position $\mathbf{r}'$ from the center of colloidal particle, while other two terms result from the induced surface charge.[63,64] Note that the Green function is invariant under the exchange of the source and the observation points $\mathbf{r} \leftrightarrow \mathbf{r}'$. Equation (1) is exact in the limit $\epsilon_c/\epsilon_w \rightarrow 0$, $\gamma = 1$. Furthermore, it was shown that it remains very accurate for $\epsilon_c/\epsilon_w \ll 1$,[61] which is appropriate for the present system with $\epsilon_c/\epsilon_w = 2.5/80$.

The expression in Eq. (1) is derived specifically for a spherical colloidal particle. To account for dielectric polarization in more complex geometries, one would need to resort to numerical boundary-element methods, such as the Iterative Dielectric Solver (IDS),[55] which is much more computationally intensive.

The electrostatic energy of the system is

$$U = \gamma\sum_{i=1}^{N}\left[\frac{q^2 a}{2\epsilon_w\left(r_i^2 - a^2\right)} + \frac{q\psi_{self}(\mathbf{r_i})}{2}\right] + \sum_{i=1}^{N-1}\sum_{j=i+1}^{N} q_i q_j G(\mathbf{r_i},\mathbf{r_j}), \tag{3}$$

where N is the total number of particles inside the cell, including the charged surface sites. The term in the square brackets is due to self-interaction of an ion with its own induced surface charge and is given by

$$\psi_{self}(\mathbf{r_i}) = \frac{q}{\epsilon_w a}\ln\left(1 - \frac{a^2}{r_i^2}\right). \tag{4}$$

Hard-sphere interactions between ions are not included in (3). Configurations with overlapping hard spheres are not allowed. Since the hydrated size of all ions is the same, H_3O^+ and K^+ are identical. The difference between the two ions is that H_3O^+ can react with acidic groups. When reacting, it transfers its charge to them, while the remaining neutral hard-sphere disappears. This is physically justifiable since the hard-sphere in our model represents a hydrated structure, which vanishes upon the proton transfer.

III. SIMULATION METHOD

The simulations are performed in the semi-grand canonical ensemble in which the system is in contact with an infinite reservoir of strong acid and salt. Since the WS cell represents an infinite colloidal suspension at finite concentration, we may think of it as being separated from the reservoir by a semipermeable membrane, which allows for a free passage of ions but not of colloidal particles. The diffusion of ions will result in an electric field across the membrane, establishing a potential difference between the system and the reservoir. This is known as the Donnan potential, φ_D. When an ion moves from the reservoir into the system it will, therefore, gain additional energy $q_i\varphi_D$.

Our reactive Monte Carlo involves two types of movements. The standard grand canonical insertion/deletion of ions between the reservoir and the simulation cell, and protonation and deprotonation moves for the surface sites. The grand canonical acceptance probabilities for insertion or deletion of an ion of type i are given by $ACC = \min\left(1, \phi_{add/rem}\right)$, where $\phi_{add/rem}$ is

$$\begin{aligned}\phi_{add} &= \frac{Vc_i}{N_i+1}\exp[-\beta(\Delta E_{ele} - \mu_{ex} + q_i\varphi_D)],\\ \phi_{rem} &= \frac{N_i}{Vc_i}\exp[-\beta(\Delta E_{ele} + \mu_{ex} - q_i\varphi_D)].\end{aligned} \tag{5}$$

Here, ΔE_{ele} is the change in electrostatic energy upon insertion or deletion of an ion, c_i is the concentration of ion of type i in the reservoir, μ_{ex} is the excess chemical potential of ions in the reservoir, and V is the free volume accessible to the ions. Note that since all ions are assumed to have the same radius and are all monovalent, the excess chemical potential of all ions is the same. The Donnan potential φ_D has to be adjusted each few MC steps to keep charge neutrality inside the system.[65] This makes simulations slow. A simple solution to this problem is to perform insertion or deletion of cations–anion pairs so that the charge neutrality of the cell is always preserved. For example, the probability of insertion/deletion of KCl pair is the product $\phi^{K^+}_{add/rem}\phi^{Cl^-}_{add/rem}$ so that the Donnan potential cancels out.

In the grand canonical ensemble, concentrations are controlled indirectly via chemical potentials. One way to establish the correspondence between μ_{ex} and the ionic concentrations is to run simulations for a bulk solution at a given concentration and then compute μ_{ex} using, for example, the Widom insertion procedure. Alternatively, one can perform a grand canonical MC with fixed chemical potentials and observe the corresponding concentration of ions inside the simulation box. We note, however, that our ionic solution is a restricted primitive model. We can, therefore, take advantage of this fact and use an accurate analytical approximation for the excess chemical potential given by $\mu_{ex} = \mu_{CS} + \mu_{MSA}$, where $\beta\mu_{CS} = \frac{8\eta - 9\eta^2 + 3\eta^3}{(1-\eta)^3}$ is the Carnahan–Starling expression for the excluded volume contribution,[66–69] where the volume fraction is $\eta = \frac{\pi d^3}{3}c_t$, d is the ionic diameter, and $c_t = c_s + c_a$ is the total concentration of salt and acid. The electrostatic contribution to the excess chemical potential can be accurately calculated using the mean spherical approximation (MSA),[70–75]

$$\beta\mu_{MSA} = \frac{\lambda_B\left(\sqrt{1+2\kappa d} - \kappa d - 1\right)}{d^2\kappa}, \tag{6}$$

where $\lambda_B = q^2/\epsilon_w k_B T$ is the Bjerrum length, and $\kappa = \sqrt{8\pi\lambda_B c_t}$ is the inverse Debye length.

To test this procedure, we choose concentrations of acid and salt from which we calculate μ_{ex} using the analytical expressions above. We then run a grand canonical MC simulation for this value of μ_{ex}, starting with an empty simulation cell. If the approximate expression for μ_{ex} is accurate, once the simulation is converged, we should recover the concentration of acid and salt inside the simulation cell that we specified to calculate μ_{ex}. This is precisely what is observed in the simulations (see Fig. 2) justifying the use of the analytical expression for μ_{ex}.

To obtain the MC weights for protonation/deprotonation moves, we first consider the free energy change for a reaction of a hydronium ion with an isolated weak acid group A^-, $H_3O^+ + A^- \rightleftharpoons HA + H_2O$. We can think of this process as a removal of a hydronium ion from the reservoir, followed by a reaction with a A^- group. The internal partition function of the HA molecule is $K_{eq}/\Lambda^3_{H^+}$, where K_{eq} is the equilibrium constant and Λ_{H^+} is the hydronium's de Broglie thermal wavelength. The free energy change of the system + reservoir resulting from the removal of a hydronium ion from the reservoir and bringing it into vicinity of A^-, where it will undergo a proton transfer reaction, is then $\beta\Delta F_p = -\ln(K_{eq}/\Lambda^3_{H^+}) - \mu_{H^+}$, where $\beta\mu_{H^+} = \ln(c_{H^+}\Lambda^3_{H^+}) + \beta\mu_{ex}$ is the total chemical potential of a hydronium ion inside the reservoir. For the deprotonation reaction, the free energy change is $\Delta F_d = -\Delta F_p$. The acceptance probabilities for protonation and deprotonation moves are, therefore,

$$\begin{aligned}\phi_p &= \exp[-\beta(\Delta E_{ele} + \Delta F_p + q\varphi_D)],\\ \phi_d &= \exp[-\beta(\Delta E_{ele} + \Delta F_d - q\varphi_D)],\end{aligned} \tag{7}$$

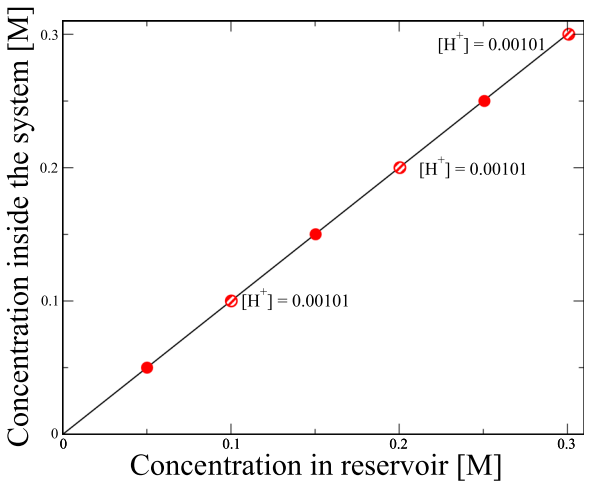

FIG. 2. Salt concentration inside the system as a function of the reservoir concentration. The reservoir also contains strong acid at concentration $c_a = 0.001$M. The straight line indicates the theoretical expectation that the concentrations of ions inside the system should be exactly the same as the concentration of ions in the reservoir. The concentration of hydronium ion inside the system is indicated next to the symbols. The excellent agreement between concentrations inside the system and in the reservoir indicates the accuracy of our expression for μ_{ex}.

respectively. These simplify to

$$\phi_p = c_{H^+} K_{eq} \exp[-\beta(\Delta E_{ele} - \mu_{ex} + q\varphi_D)],$$
$$\phi_d = \frac{1}{c_{H^+} K_{eq}} \exp[-\beta(\Delta E_{ele} + \mu_{ex} - q\varphi_D)]. \quad (8)$$

A Monte Carlo "reaction" move consists of selecting a random titration site, followed by an attempt to change its "state" from protonated to deprotonated and vice versa. Note that the acceptance probabilities depend on the Donnan potential, which is *a priori*, unknown. We can overcome this difficulty by again combining a protonation attempt with insertion of Cl^-. The probability of acceptance of a protonation-Cl^--insertion move is then $\min\{1, \phi_p \phi_{add}\}$. In the product, the Donnan potential once again cancels out. Similarly, a deprotonation move is combined with removal of Cl^- so that the probability is $\min\{1, \phi_d \phi_{rem}\}$. The final acceptance probabilities for the pair moves are

$$\phi_{d+rem} = \frac{N_{Cl^-}}{c_{H^+} K_{eq} V c_{Cl^-}} \exp[-\beta(\Delta E_{ele} + 2\mu_{ex})],$$
$$\phi_{p+add} = \frac{c_{H^+} K_{eq} V c_{Cl^-}}{(N_{Cl^-} + 1)} \exp[-\beta(\Delta E_{ele} - 2\mu_{ex})], \quad (9)$$

where N_{Cl^-} is the number of Cl^- ions inside the cell. In Fig. 1, we have schematically shown these movements.

IV. COMPARISON WITH THE EXPERIMENTAL RESULTS

We now apply the simulation method discussed above to study the effective charge of carboxyl latex particles,[76] the surface sites of which undergo reaction $COOH \rightleftharpoons COO^- + H^+$. The simulated system consists of a spherical cell of radius $R = 120$ Å, with a spherical colloidal particle at the center, represented by a hard-sphere of radius $a = 60$ Å, with surface titration sites of $r_0 = 2$ Å (see Fig. 1).

The mobile ions correspond to the dissociation of KCl and HCl. We are interested in obtaining the effective charge of a colloidal particle as a function of pH and salt concentrations in the reservoir. Recall that $pH = -\log[a_{H^+}]$, where $a_{H^+} = c_{H^+} \exp[\beta\mu_{ex}(c_t)]$ is the activity of hydronium ions. Furthermore, the electrochemical potential of an ion inside the system and in the reservoir is the same. Recall that inside the simulation cell, the electrochemical potential of an ion includes the Donnan potential. This means that the activity of hydronium ion is the same inside the cell, and in the reservoir, therefore, pH inside the simulation cell and the reservoir is the same.

We consider two different carboxyl latex colloidal particles, the effective charge of which has been obtained experimentally using potentiometric titration.[76] It is important to remember that the surface association constant K_{eq} is different from the bulk association constant for the same acid.[77–82] This difference may be attributed to the distinct symmetry of the electronic wave function of a chemical group when it is on the surface of a colloidal particle and when it is in the bulk. Our strategy, then, is to adjust K_{eq} to fit the experimental titration curve for colloidal particles with the bare surface charge density $\sigma_T = 78$ mC/m^2, amounting to 220 titration sites randomly distributed over the colloidal surface, inside the electrolyte solution of $c_{KCl} = 10$ mM. We will then use the *same* K_{eq} to calculate the theoretical titration curves for other salt concentrations and different colloidal bare charges. Recalling that acid dissociation constant is $K_a = 1/K_{eq}$, we obtain an excellent fit of the experimental titration curve using $pK_a = -\log[K_a] = \log[K_{eq}] = 5.02$ [see Fig. 3(a)]. This value is actually very close to pK_a of bulk acetic acid. We next use

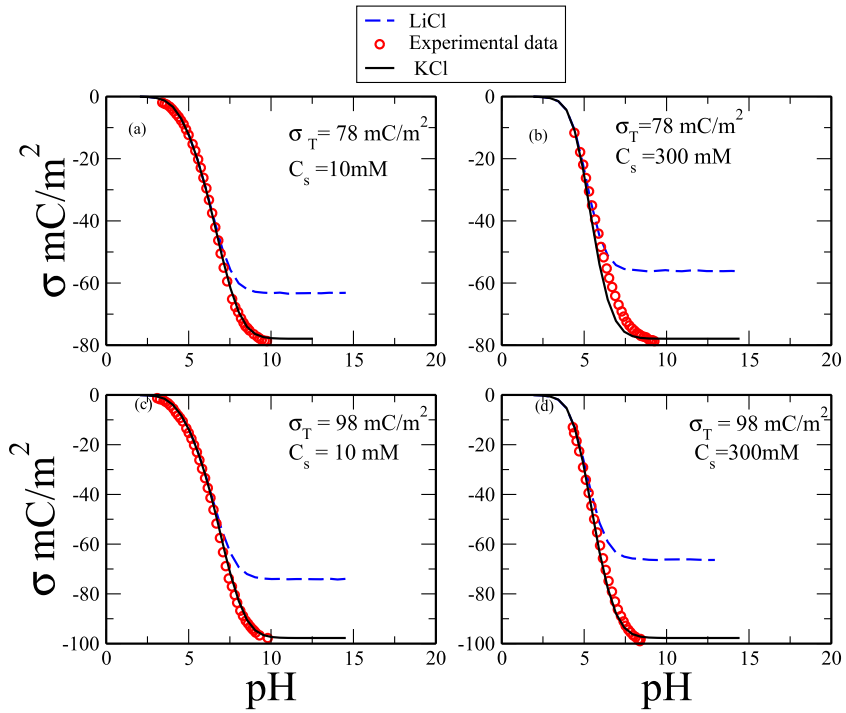

FIG. 3. Effective charge obtained using the reactive MC simulations (curves) compared with the experimental data (circles). The solid black curve is the effective charge in the presence of KCl and the dashed blue curve in the presence of LiCl. The bare surface charge densities of colloidal particles are 78 mC/m^2 [panels (a) and (b)] and 98 mC/m^2 [panels (c) and (d)]. Electrolyte concentration is indicated in each panel. The surface equilibrium constant, $pK_a = 5.02$, is obtained by fitting the experimental data in panel (a). The *same* equilibrium constant is then used to calculate the effective charges for other salt concentrations and colloidal bare charge [panels (b)–(d)]. A good agreement is observed between theory and experiment.[76]

the same value of pK_a to calculate the titration curve for a particle of the same bare surface charge inside an electrolyte solution of 300 mM. Only a reasonable agreement between experiment and theory is obtained for this case [Fig. 3(b)] with a significant deviation appearing at large pH. Finally, we calculate the titration curves for colloidal particles of surface charge $\sigma_T = 98$ mC/m^2, in solutions of 10 and 300 mM electrolyte, using the *same* surface equilibrium constant as before. A good agreement is found between simulations and experiments for both of these concentrations of electrolyte [see Figs. 3(c) and 3(d)]. At the moment, we do not have a clear understanding of what is the cause of the deviation between theory and experiment observed for particles of surface charge $\sigma_T = 78$ mC/m^2 inside 300 mM electrolyte solution. The deviation is particularly surprising in view of the fact that for $\sigma_T = 98$ mC/m^2 and 300 mM electrolyte, we do have a good agreement between theory and experiment.

We should note that in our simulation, the size of colloidal particles is much smaller than in the experiment. We have checked, however, that this does not affect the titration curve, as long as the charge density of the particles is the same. Similarly, our calculations are performed for colloidal suspension at finite volume fraction, while experiments were done at infinite dilution. Again the size of the WS cell does not affect the titration curve, as long as the cell is sufficiently large. To demonstrate this, in Fig. 4 we present the titration curve for particles with bare surface charge density 98 mC/m^2 inside two different WS cells of radius 120 and 200 Å. The two titration curves are practically indistinguishable. This shows that the effective colloidal charge does not depend on the volume fraction for sufficiently dilute suspensions.

In biochemistry and analytical chemistry, pK_a is usually calculated using the Henderson–Hasselbalch (HH) equation that relates pK_a to the pH, when half of acidic groups are titrated. For our system, the HH equation can be written as

$$pK_a^{HH} = pH_{1/2} + \beta q \varphi \log_{10}(e), \tag{10}$$

where e is the Euler number and φ is the mean electrostatic potential at the center of an adsorption site produced by all the other sites and ions inside the simulation cell at pH = $pH_{1/2}$, when half of the surface acidic group are titrated. The value of $pH_{1/2}$ can be read directly from Fig. 3. In Table I, we compared the value of pK_a^{HH} obtained using the HH equation with the "exact" microscopic $pK_a = 5.02$ used to calculate the titration curve in our reactive MC simulation. We see that pK_a^{HH} values calculated using the HH equation do not agree exactly with $pK_a = 5.02$ used to obtain all the titration curves in our MC simulations. This is not particularly surprising since the HH is a mean-field equation, which does not fully account for the electrostatic correlations between the ions and between ions and sites.[83]

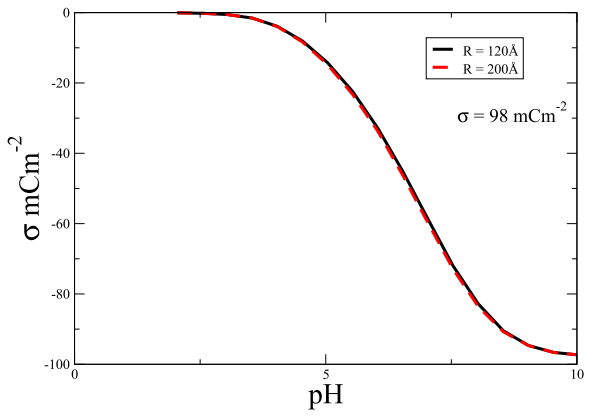

FIG. 4. Titration curves for a particle with surface charge density 98 mC/m^2 inside two different WS cells.

TABLE I. The values of pK_a^{HH} calculated using the HH equation for different colloidal particles and salt concentrations. The "microscopic" pK_a used to obtain all the titration curves in the simulations was $pK_a = 5.02$.

σ (mCm^{-2})	KCl (mM)	pK_a^{HH}	$pH_{1/2}$
78	10	5.47	6.4
78	300	5.25	5.4
98	10	5.31	6.7
98	300	5.32	5.5

V. SPECIFIC ION ADSORPTION

The specific ion adsorption can be easily incorporated within the simulation formalism introduced above. It is known that Li^+ ion can specifically associate with COO^-.[84,85] We are, therefore, interested to explore the effect of replacing KCl with LiCl salt. The specific association of Li^+ with COO^- is a consequence of the law of matching water affinities (LMWA),[86] which suggests that both lithium and carboxylate can lose part of their hydration sheath resulting in strong electrostatic interaction between the two ions.[87–92] Based on the LMWA, we will take the distance of the closest approach between lithium and carboxylate contact pair to be $d = 2.9$ Å, corresponding to the Latimer diameter of Li^+ ion.[93,94] We can then say that any lithium ion that is within the distance $d = 5.3$ Å—the separation distance between a fully hydrated Li^+ and the adsorption site—is associated with the carboxylate group and will contribute to the renormalization of the effective colloidal charge.

In Fig. 3 (dashed blue curves), we show the effect of replacing K^+ with Li^+ on the effective colloidal charge. Note the saturation of colloidal charge at large pH, resulting from the association of Li^+ ions with the carboxylate groups. Specific adsorption of Li^+ also affects the protonation of carboxylate, although the effect appears to be quite small (see Fig. 5). We expect to see a more significant effect if Li^+ is replaced by divalent Ca^{++} ion, which is known to strongly interact with the carboxylate. This will be explored in future work.

The degree of protonation for the same pH is lower in the case of LiCl compared to KCl salt, since Li^+ ion effectively competes with H^+ for acidic sites. Although deprotonation is larger for LiCl, this does not imply that the effective colloidal surface charge is also larger. Adsorbed Li^+ ions neutralize sites similarly to H^+ and, therefore, contributed to the effective charge of colloidal particles. Thus, the effective surface charge of colloidal particles in the case of LiCl solutions is lower in modulus compared to solutions of KCl, for which no specific association takes place (see Fig. 3). Again, we expect the effect of specific associations to be even more important for suspensions containing $CaCl_2$.

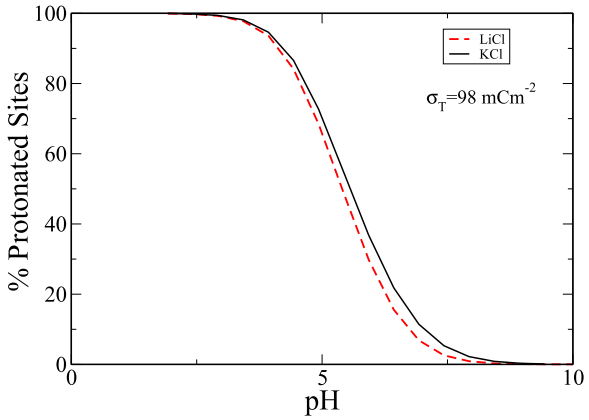

FIG. 5. The fraction of protonated groups in the presence of 300 mM of either KCl or LiCl salts. Specific adsorption of Li^+ to carboxylate groups results in stronger deprotonation, in particular, at larger pH values.

VI. CONCLUSIONS

We have presented a simulation method that allows us to very accurately calculate the titration curves for suspensions of colloidal particles. The results were compared with the experimental measurements of the effective colloidal charge obtained using potentiometric titration. A good agreement was found between simulations and experiments. We have also shown how the specific ion interaction, responsible for the Hofmeister effect, can be easily included in our simulation method. The approach presented in this paper can also be applied to other scientifically and technologically important systems, such as proteins, polyelectrolyte gels, and polyampholytes.

ACKNOWLEDGMENTS

This work was partially supported by the CNPq, the CAPES, and the National Institute of Science and Technology Complex Fluids INCT-FCx. The authors are grateful to the Instituto de Física e Matemática, UFPel, for the use of computer resources. D.F. acknowledges financial support from the FONDECYT through Grant No. 1201192.

AUTHOR DECLARATIONS

Conflict of Interest

The authors have no conflicts to disclose.

DATA AVAILABILITY

The data that support the findings of this study are available from the corresponding author upon reasonable request.

REFERENCES

[1] D. Prusty, R. J. Nap, I. Szleifer, and M. Olvera de la Cruz, Soft Matter **16**, 8832 (2020).
[2] C.-Y. Leung, L. C. Palmer, S. Kewalramani, B. Qiao, S. I. Stupp, M. Olvera de la Cruz, and M. J. Bedzyk, Proc. Natl. Acad. Sci. U. S. A. **110**, 16309 (2013).
[3] L. Javidpour, A. Božič, A. Naji, and R. Podgornik, Soft Matter **17**, 4296 (2021).
[4] L. Javidpour, A. L. Božič, R. Podgornik, and A. Naji, Sci. Rep. **9**, 3884 (2019).
[5] L. Fink, C. Allolio, J. Feitelson, C. Tamburu, D. Harries, and U. Raviv, Langmuir **36**, 10715 (2020).
[6] A. Kubincová, P. H. Hünenberger, and M. Krishnan, J. Chem. Phys. **152**, 104713 (2020).
[7] M. Krishnan, J. Chem. Phys. **146**, 205101 (2017).
[8] M. Krishnan, J. Chem. Phys. **138**, 114906 (2013).
[9] A. Behjatian, M. Bespalova, N. Karedla, and M. Krishnan, Phys. Rev. E **102**, 042607 (2020).
[10] B. Ma and M. Olvera de la Cruz, J. Phys. Chem. B **125**, 3015 (2021).
[11] C. Gao, S. Kewalramani, D. M. Valencia, H. Li, J. M. McCourt, M. Olvera de la Cruz, and M. J. Bedzyk, Proc. Natl. Acad. Sci. U. S. A. **116**, 22030 (2019).
[12] Y. Avni, R. Podgornik, and D. Andelman, J. Chem. Phys. **153**, 024901 (2020).
[13] Y. Avni, D. Andelman, and R. Podgornik, Curr. Opin. Electrochem. **13**, 70 (2019).
[14] R. M. Adar, D. Andelman, and H. Diamant, Adv. Colloid Interface Sci. **247**, 198 (2017), part of the Special Issue: Dominique Langevin Festschrift: Four Decades Opening Gates in Colloid and Interface Science.
[15] H. Shen and D. D. Frey, J. Chromatogr. A **1079**, 92 (2005).
[16] H.-K. Tsao, Langmuir **16**, 7200 (2000).
[17] H. Löwen, A. Esztermann, A. Wysocki, E. Allahyarov, R. Messina, A. Jusufi, N. Hoffmann, D. Gottwald, G. Kahl, and M. Konieczny, J. Phys.: Conf. Ser. **11**, 207 (2005).
[18] R. Messina, C. Holm, and K. Kremer, J. Chem. Phys. **117**, 2947 (2002).
[19] R. Messina, C. Holm, and K. Kremer, Comput. Phys. Commun. **147**, 282 (2002), part of the Special Issue: Proceedings of the Europhysics Conference on Computational Physics Computational Modeling and Simulation of Complex Systems.
[20] M. Borkovec, B. Jönsson, and G. J. M. Koper, "Ionization processes and proton binding in polyprotic systems: Small molecules, proteins, interfaces, and polyelectrolytes," in *Surface and Colloid Science*, edited by E. Matijević (Springer, Boston, 2001), pp. 99–339.
[21] C. F. Narambuena, P. M. Blanco, A. Rodriguez, D. E. Rodriguez, S. Madurga, J. L. Garcés, and F. Mas, Polymer **212**, 123170 (2021).
[22] I. Worms, D. F. Simon, C. S. Hassler, and K. J. Wilkinson, Biochimie **88**, 1721 (2006).
[23] I. R. Booth, Microbiol. Rev. **49**, 359 (1985).
[24] J. Antelo, M. Avena, S. Fiol, R. López, and F. Arce, J. Colloid Interface Sci. **285**, 476 (2005).
[25] M. Brigante and M. Avena, Microporous Mesoporous Mater. **225**, 534 (2016).
[26] F. Hammes and W. Verstraete, Rev. Environ. Sci. Biotechnol. **1**, 3 (2002).
[27] A. A. R. Teixeira, M. Lund, and F. L. Barroso da Silva, J. Chem. Theory Comput. **6**, 3259 (2010).
[28] A. Kurkdjian and J. Guern, Annu. Rev. Plant Physiol. Plant Mol. Biol. **40**, 271 (1989).
[29] A. Accardi and C. Miller, Nature **427**, 803 (2004).
[30] T. J. Beveridge, Annu. Rev. Microbiol. **43**, 147 (1989).
[31] A. van der Wal, W. Norde, A. J. B. Zehnder, and J. Lyklema, Colloids Surf., B **9**, 81 (1997).
[32] H. T. M. Heinrich, P. J. Bremer, C. J. Daughney, and A. J. McQuillan, Langmuir **23**, 2731 (2007).
[33] B. C. Pressman, Proc. Natl. Acad. Sci. U. S. A. **53**, 1076 (1965).
[34] M. Lund and B. Jönsson, Q. Rev. Biophys. **46**, 265 (2013).
[35] R. Lunkad, A. Murmiliuk, P. Hebbeker, M. Boublík, Z. Tošner, M. ŠtĚpánek, and P. Košovan, Mol. Syst. Des. Eng. **6**, 122 (2021).
[36] R. Lunkad, A. Murmiliuk, Z. Tošner, M. ŠtĚpánek, and P. Košovan, Polymers **13**, 214 (2021).
[37] M. F. Perutz, Science **201**, 1187 (1978).
[38] B. Svensson, B. Jönsson, and C. Woodward, Biophys. Chem. **38**, 179 (1990).
[39] C. E. Woodward and B. R. Svensson, J. Phys. Chem. **95**, 7471 (1991).
[40] M. Lund and B. Jönsson, Biochemistry **44**, 5722 (2005).
[41] E. Dickinson and M. E. Leser, *Food Colloids: Self-Assembly and Material Science* (Royal Society of Chemistry, 2007).
[42] F. L. B. da Silva and B. Jönsson, Soft Matter **5**, 2862 (2009).
[43] K. Szuttor, F. Weik, J.-N. Grad, and C. Holm, J. Chem. Phys. **154**, 054901 (2021).

[44]S. H. Behrens and D. G. Grier, J. Chem. Phys. **115**, 6716 (2001).
[45]M. Lund, T. Åkesson, and B. Jönsson, Langmuir **21**, 8385 (2005).
[46]D. Andelman, in *Soft Condensed Matter Physics in Molecular and Cell Biology*, edited by W. C. Poon and D. Andelman (Taylor & Francis, New York, 2006), Vol. 6, p. 96.
[47]R. Podgornik, J. Chem. Phys. **149**, 104701 (2018).
[48]S. Madurga, C. Rey-Castro, I. Pastor, E. Vilaseca, C. David, J. L. Garcés, J. Puy, and F. Mas, J. Chem. Phys. **135**, 184103 (2011).
[49]T. Nishio, Biophys. Chem. **57**, 261 (1996).
[50]T. Nishio, Biophys. Chem. **49**, 201 (1994).
[51]J. K. Johnson, A. Z. Panagiotopoulos, and K. E. Gubbins, Mol. Phys. **81**, 717 (1994).
[52]J. P. Valleau and L. K. Cohen, J. Chem. Phys. **72**, 5935 (1980).
[53]J. Landsgesell, P. Hebbeker, O. Rud, R. Lunkad, P. Košovan, and C. Holm, Macromolecules **53**, 3007 (2020).
[54]F. Grünewald, P. C. T. Souza, H. Abdizadeh, J. Barnoud, A. H. de Vries, and S. J. Marrink, J. Chem. Phys. **153**, 024118 (2020).
[55]T. Curk and E. Luijten, Phys. Rev. Lett. **126**, 138003 (2021).
[56]M. Stornes, P. M. Blanco, and R. S. Dias, Colloids Surf., A **628**, 127258 (2021).
[57]S. Madurga, J. L. Garcés, E. Companys, C. Rey-Castro, J. Salvador, J. Galceran, E. Vilaseca, J. Puy, and F. Mas, Theor. Chem. Acc. **123**, 127 (2009).
[58]H. Wennerström, B. Jönsson, and P. Linse, J. Chem. Phys. **76**, 4665 (1982).
[59]E. R. Nightingale, Jr., J. Phys. Chem. **63**, 1381 (1959).
[60]A. Bakhshandeh, A. P. Dos Santos, and Y. Levin, Phys. Rev. Lett. **107**, 107801 (2011).
[61]A. P. dos Santos, A. Bakhshandeh, and Y. Levin, J. Chem. Phys. **135**, 044124 (2011).
[62]A. Bakhshandeh, Chem. Phys. **513**, 195 (2018).
[63]W. T. Norris, IEE Proc.: Sci., Meas. Technol. **142**, 142 (1995).
[64]I. V. Lindell, Am. J. Phys. **61**, 39 (1993).
[65]S. A. Barr and A. Z. Panagiotopoulos, Phys. Rev. E **86**, 016703 (2012).
[66]N. F. Carnahan and K. E. Starling, J. Chem. Phys. **51**, 635 (1969).
[67]N. F. Carnahan and K. E. Starling, J. Chem. Phys. **53**, 600 (1970).
[68]D. J. Adams, Mol. Phys. **28**, 1241 (1974).
[69]J. C. d. S. L. Maciel, C. R. A. Abreu, and F. W. Tavares, Braz. J. Chem. Eng. **35**, 277 (2018).
[70]J. S. Høye and E. Lomba, J. Chem. Phys. **88**, 5790 (1988).
[71]C.-H. Ho, H.-K. Tsao, and Y.-J. Sheng, J. Chem. Phys. **119**, 2369 (2003).
[72]Y. Levin and M. E. Fisher, Physica A **225**, 164 (1996).
[73]E. Waisman and J. L. Lebowitz, J. Chem. Phys. **56**, 3086 (1972).
[74]E. Waisman and J. L. Lebowitz, J. Chem. Phys. **56**, 3093 (1972).
[75]L. Blum, Mol. Phys. **30**, 1529 (1975).
[76]S. H. Behrens, D. I. Christl, R. Emmerzael, P. Schurtenberger, and M. Borkovec, Langmuir **16**, 2566 (2000).
[77]J. Buffle and R. A. Chalmers, *Complexation Reactions in Aquatic Systems* (John Wiley & Sons, Inc., New York, 1988).
[78]E. D. Cera, *Thermodynamic Theory of Site-Specific Binding Processes in Biological Macromolecules* (Cambridge University Press, 1995).
[79]J. Lluís Garcés, F. Mas, J. Puy, J. Galceran, and J. Salvador, J. Chem. Soc., Faraday Trans. **94**, 2783 (1998).
[80]A. Bakhshandeh, D. Frydel, A. Diehl, and Y. Levin, Phys. Rev. Lett. **123**, 208004 (2019).
[81]A. Bakhshandeh, D. Frydel, and Y. Levin, Phys. Chem. Chem. Phys. **22**, 24712 (2020).
[82]D. A. Gomez, D. Frydel, and Y. Levin, J. Chem. Phys. **154**, 074706 (2021).
[83]Y. Levin, Rep. Prog. Phys. **65**, 1577 (2002).
[84]J. S. Uejio, C. P. Schwartz, A. M. Duffin, W. S. Drisdell, R. C. Cohen, and R. J. Saykally, Proc. Natl. Acad. Sci. U. S. A. **105**, 6809 (2008).
[85]A. Sthoer, J. Hladílková, M. Lund, and E. Tyrode, Phys. Chem. Chem. Phys. **21**, 11329 (2019).
[86]K. D. Collins, Biophys. Chem. **167**, 43 (2012).
[87]J. Iwahara, A. Esadze, and L. Zandarashvili, Biomolecules **5**, 2435 (2015).
[88]S. Winstein, P. E. Klinedinst, Jr., and E. Clippinger, J. Am. Chem. Soc. **83**, 4986 (1961).
[89]M. T. Record, Jr., T. M. Lohman, and P. d. Haseth, J. Mol. Biol. **107**, 145 (1976).
[90]J.-M. Lü, S. V. Rosokha, S. V. Lindeman, I. S. Neretin, and J. K. Kochi, J. Am. Chem. Soc. **127**, 1797 (2005).
[91]J. M. Masnovi and J. K. Kochi, J. Am. Chem. Soc. **107**, 7880 (1985).
[92]T. Yabe and J. K. Kochi, J. Am. Chem. Soc. **114**, 4491 (1992).
[93]A. Diehl, A. P. Dos Santos, and Y. Levin, J. Phys.: Condens. Matter **24**, 284115 (2012).
[94]W. M. Latimer, K. S. Pitzer, and C. M. Slansky, *Molecular Structure and Statistical Thermodynamics: Selected Papers of Kenneth S. Pitzer* (World Scientific, 1993), pp. 485–489.